Spatial Reaction Engineering Approach as an Alternative for Nonequilibrium Multiphase Mass-Transfer Model for Drying of Food and Biological Materials

Aditya Putranto
Dept. of Chemical Engineering, Monash University, Clayton Campus, Melbourne, Victoria 3800, Australia

Xiao Dong Chen
Dept. of Chemical and Biochemical Engineering, College of Chemistry and Chemical Engineering, Xiamen University, Xiamen, Fujian Province, People's Republic of China

DOI 10.1002/aic.13808
Published online April 17, 2012 in Wiley Online Library (wileyonlinelibrary.com).

Drying is a complex process which involves simultaneous heat and mass transfer. Complicated structure and heterogeneity of food and biological materials add to the complexity of drying. Drying models are important for improving dryer design and for evaluating dryer performance. The lumped reaction engineering approach (L-REA) has been shown to be an accurate and robust alternative for cost-effective simulations of challenging drying systems. However, more insightful physics has to be shown spatially. In this study, the REA is coupled with the standard mechanistic drying models to yield the spatial-REA (S-REA) as nonequilibrium multiphase mass-transfer model. The S-REA consists of a system of equations of conservation with the REA representing the local evaporation and wetting rate. Results of the modeling using the S-REA match well with the experimental data reported previously. This is the first comprehensive REA approach to model the profiles of water vapor concentration during drying of food and biological materials. This study indicates that the S-REA can be an accurate nonequilibrium multiphase mass-transfer model with appropriate account of the local evaporation rate. The overall REA concept is expected to contribute substantially for better and cost-effective representation of transport phenomena of drying process. © 2012 American Institute of Chemical Engineers *AIChE J,* 59: 55–67, 2013
Keywords: S-REA, convective drying, food and biological materials, modeling, multiphase, nonequilibrium

Introduction

Food and biological materials are highly perishable because of the high water content and biological nature. Several chemical and biochemical changes may occur during storage and transportation. To retard the changes, drying has long been recognized as one of the most effective ways to maintain food and biological product quality. The lower water content inside the product can lengthen the storage life, while minimizing the transportation costs.

Drying involves simultaneous heat and mass transfer. Studies of drying are important for process and equipment design, and product technology perspectives. Drying is usually energy intensive process, in particular, when hot air is used to evaporate the water contained in the product. Because of the rise of climate change issues, sustainable drying techniques are desirable. Intermittent drying, as an example for more efficient operation, is recently applied by supplying time-varying heat input during drying period. It has been shown to be effective in reducing drying time and energy, yet resulting in similar final moisture content.[1–5] Drying may affect product quality; for example, nonenzymatic browning, ascorbic acid loss, beta carotene reduction, fissuring, and cracking were reported to be closely associated with drying. Appropriate drying schemes need be identified to maintain the quality during drying.[1,2,6–10]

A reliable drying model is extremely useful for exploring drying schemes for low energy use and high quality products. Drying models are usually classified into empirical and mechanistic models. The first ones, especially those of explicit time functions, cannot capture physics during drying and cannot be extrapolated to other conditions. These models are not appropriate as predictive tools. The mechanistic models usually use diffusion-based models and the models are represented in partial differential equation to describe the dependence of moisture content and temperature on time and position.[11–15] The diffusion-based models are often marked by the effective liquid diffusivity usually represented as function of moisture content and temperature. Many diffusion-based models have been implemented with various degree of success.[11–15]

Many of these extensive diffusion-based models implemented usually assume that "effective" liquid diffusion occurs.[16–19] Several researchers simply used effective diffusivity to represent the whole phenomenon (liquid and vapor diffusion).[20–23] Chen[24] analyzed that the effective diffusivity

Correspondence concerning this article should be addressed to X. D. Chen at xdc@xmu.edu.cn.

is actually a complex interaction of variables involved during drying including temperature, moisture content, and pressure. Crank's effective diffusivity was also generally used without necessary justification although the process of experimentally obtaining it is only valid under condition of isothermal, negligible shrinkage, and negligible external resistance.[25] For better understanding of the transport phenomena, application of effective liquid diffusion alone may not be sufficient as it cannot represent the water vapor concentration during drying which could be affected by pore structure.[24] Vapor generation and transfer may affect the other volatile transport in the same material.

Implementation of multiphase drying model with appropriate source/depletion term for better representation of transport phenomena of drying process is important as the models without the source term "generated" an anomaly.[24,26–28] This encourages the application of the multiphase drying model with source/depletion terms. For more generic application of the multiphase drying model, it is suggested that the nonequilibrium approach is perhaps more appropriate.[27] The good nonequilibrium multiphase drying model is also useful in determining the appropriateness of the equilibrium approach for the situation of concern.[27] The application of the internal evaporation/condensation rate is a crucial factor in the modeling of nonequilibrium multiphase drying.[27] The evaporation rate should be affected by both vapor and liquid transport and this is not equal to the moisture loss.[27] It is necessary to represent the internal evaporation rate explicitly and appropriately to implement this model. The internal evaporation/condensation rate is implemented in the multiphase drying model as depletion term for the liquid phase and as source term for the vapor phase. It was proposed that the internal evaporation rate can be related to the difference of equilibrium vapor pressure and the vapor pressure at particular time inside the pore spaces.[27–30]

The reaction engineering approach (REA) was first suggested by Chen (the second author) in 1996 and has been implemented to model several challenging drying systems.[31–43] The REA was shown to be accurate and robust to model convective drying of thin layer or small food materials.[31–36] The REA was also accurate in modeling drying of nonfood materials including the one with infrared-heating.[37] Application of the REA on the cyclic drying of polymer drying was shown to be successful.[38] Application of the REA has also been extended not only on the thin layer or small food materials but also on the thick sample materials. The combination of the REA and the approximation of the temperature distribution inside the sample can describe both moisture content and temperature profiles accurately for thick samples.[39,43] Recently, the REA has been applied to model the cyclic drying under time-varying humidity and temperature, the heat treatment of wood under time-varying gas temperature as well as the baking of thin cake. The results of the modeling matched well with the experimental data. This indicates that the REA is indeed flexible to model the more challenging drying systems.[40–43]

Although the nonequilibrium multiphase drying model is suggested as mentioned previously, to the best of our knowledge, there has been no nonequilibrium multiphase drying model implemented apart from the work of Kar and Chen,[44,45] which implemented the spatial-REA (S-REA) while neglecting liquid diffusion to model the convective drying of very thin porcine skin (as a model for transdermal drug delivery as influenced by moisture transfer) to demonstrate the "bottom line" of the model. The exercise there[44,45] was to see if the liquid diffusion is crucial factor in gaining physically sound profiles. It has been turned out that it predicted a concave water content that is not reasonable. Therefore, it has naturally progressed to this work which is much more complete. Here, the REA is combined with the standard mechanistic drying model to yield the nonequilibrium multiphase drying model called S-REA, which is the first model applied for nonequilibrium multiphase drying. The liquid diffusion is also incorporated based on the analysis given by Kar and Chen.[44] The S-REA is expected to describe the spatial moisture content, water vapor concentration and temperature during drying accurately and a better understanding of transport phenomena of drying process can be gained.

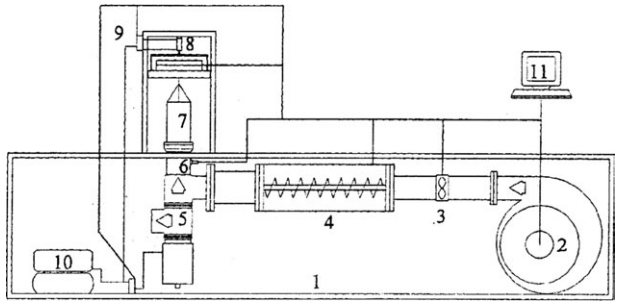

Figure 1. Drying equipment of convective drying of mango tissues.[46]

The study is aimed to implement a comprehensive REA approach, that is, the S-REA to model the convective drying of food materials. In this article, the S-REA is applied to model the convective drying of potato tissues, where appropriate experimental data are available. The applicability of the REA as the local evaporation rate as well as the accuracy and robustness of the S-REA as a candidate for nonequilibrium multiphase drying model has been investigated in this study. The outline of the article is: first, the REA is introduced to explain briefly the fundamentals of the REA followed by the explanation of the S-REA. Subsequently, the S-REA is applied to model convective drying of potato tissues, the results of the modeling and their comparison against available experimental data are presented then the relevant discussions on the applicability of the S-REA are provided.

Experimental Details

Convective drying of mango tissues

The experimental data of drying of mango tissues are derived from the previous study.[15] For better understanding of the predictions, the necessary experimental details are summarized and reviewed in this section. The experimental setup is shown in Figure 1. The samples of mango tissues were made cubes with initial side-length of 2.5 cm, while the initial moisture content and temperature were 9.3 kg kg^{-1} and 10.8°C, respectively. The laboratory drier was described in Sanjuan et al.[46] During drying, the weight change of the sample and the center temperature history were recorded. The drying air temperature and air velocity were controlled at preset values by proportional integral derivative (PID) control algorithms, whereas air humidity was maintained constant during drying. The experimental setting for convective drying is shown in Table 1. The density,

Table 1. Experimental Conditions of Convective Drying of Mango Tissues[15]

Number	Air Velocity (m s^{-1})	Air Temperature (°C)	Air Humidity (kg H_2O kg dry air^{-1})
1	4	45	0.0134
2	4	55	0.0134
3	4	65	0.0134

thermal conductivity, heat capacity, equilibrium moisture content, and shrinkage of the samples are presented in previous publication.[43]

Convective drying of potato tissues

The experimental data on drying of potato tissues used were taken from the previous work.[47] Their experimental details are also reviewed here for better understanding of the modeling approach.[47–49] The cylindrical samples of Russet potatoes with diameters of 1.4 and 2.8 cm were obtained using cylindrical cutters. The samples were sealed at top and bottom ends with epoxy to establish approximately a one-dimensional (1-D) (radial direction) moisture transfer. The experiments were conducted in a laboratory convective dryer with the drying air temperature of 70°C and axial velocity of 1.5 m s^{-1}. The experimental setup is shown in Figure 2.[48] The fan at the bottom of the sample draws air downward and this reduces the turbulence effect near the sample as the air moves downward.[49] The position of thermocouples inside the samples is shown in Figure 3. The samples with the diameter of 1.4 cm were cut into two concentric parts for measurement of moisture content distribution, that is, core and cortex (the core is a cylinder with the radius of 0.35 cm derived from the inner part of the potato tissues, whereas the cortex is a concentric shell derived from the outer part of the potato tissues). For the samples with the diameter of 2.8 cm, the samples were cut into four concentric parts, that is, core, cortex 1, cortex 2, and cortex 3. Similar to the samples with the diameter of 1.4 cm, the core is a cylinder with the radius of 0.35 cm derived from the innermost part of the potato tissues. The procedures were repeated for a number of intervals.[47] The physical properties of potato tissues are shown in Appendix A.

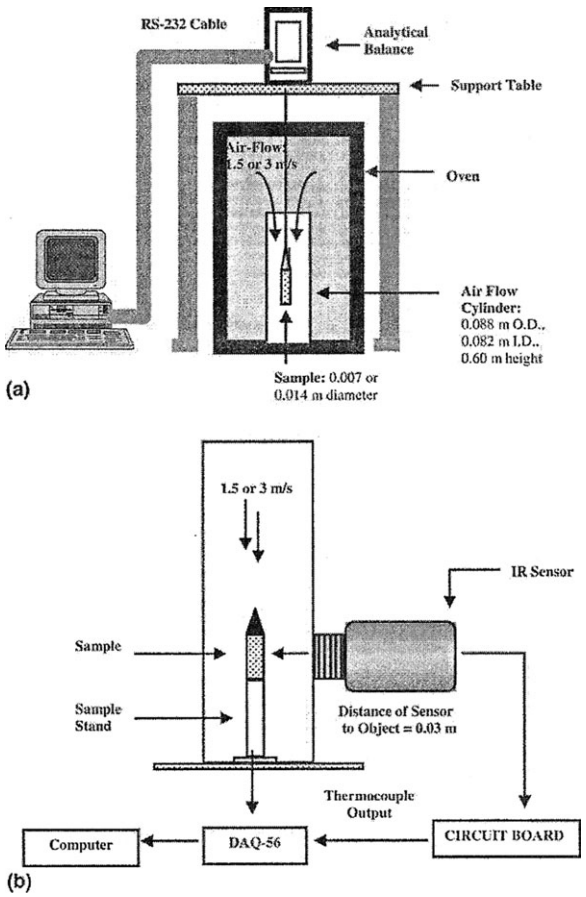

Figure 2. Experimental setup of convective drying of potato tissues.[48]

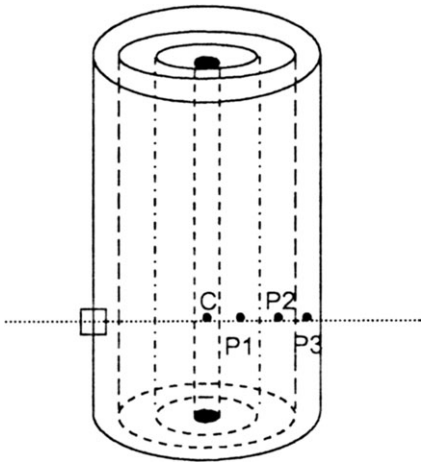

Figure 3. Core and cortex of potato tissues with diameter of 2.8 cm.[47]

Brief Review of the Reaction Engineering Approach

The general REA is an application of chemical reaction engineering principles to model drying kinetics which was first reported in 1997.[31,50] A summary of the developments of the REA, in particular, the lumped approach of REA, was given by Chen.[50]

In general, with no assumption, the drying rate of a material can be expressed as

$$m_s \frac{d\overline{X}}{dt} = -h_m A(\rho_{v,s} - \rho_{v,b}) \tag{1}$$

Equation 1 is a basic mass-transfer equation. The convective mass-transfer coefficient (h_m) is determined based on the established Sherwood number correlations for the geometry and flow condition of concern or established experimentally for the specific drying conditions involved. The surface vapor concentration ($\rho_{v,s}$) is then scaled against saturated vapor concentration ($\rho_{v,sat}$) using the following equation[31,50]

$$\rho_{v,s} = \exp\left(\frac{-\Delta E_v}{RT_s}\right)\rho_{v,sat}(T_s) \tag{2}$$

where ΔE_v represents the additional difficulty to remove moisture from the material beyond the free water effect. This ΔE_v is the moisture content (X) dependent. T_s is the surface temperature of the material being dried (K) and $\rho_{v,sat}$ for water vapor can be estimated by

$$\rho_{v,sat} = 4.844 \times 10^{-9}(T_s - 273)^4 - 1.4807 \times 10^{-7}(T_s - 273)^3 + 2.6572 \times 10^{-5}(T_s - 273)^2 - 4.8613 \times 10^{-5}(T_s - 273) + 8.342 \times 10^{-3} \quad (3)$$

Based on the data summarized by Keey,[51] where T_s is the sample surface temperature (K) used in eq. 2. When material is "thermally" thin, the surface temperature is considered to be the same as the sample temperature.[52,53] The mass balance (eq. 1) is then expressed as

$$m_s \frac{d\overline{X}}{dt} = -h_m A \left[\exp(\frac{-\Delta E_v}{RT_s}) \rho_{v,sat}(T_s) - \rho_{v,b} \right] \quad (4)$$

From eq. 4, it can be observed that the REA is expressed in the first-order ordinary differential equation with respect to time and the model is the core of the lumped-REA (L-REA). The L-REA does not assume uniform moisture content, but it evaluates average moisture content of the samples during drying.

The activation energy (ΔE_v) is determined experimentally by placing the parameters required for eq. 4 in its rearranged form

$$\Delta E_v = -RT_s \ln \left[\frac{-m_s \frac{d\overline{X}}{dt} \frac{1}{h_m A} + \rho_{v,b}}{\rho_{v,sat}} \right] \quad (5)$$

where $d\overline{X}/dt$ is experimentally determined. Besides the average moisture content, the surface area, temperature, and mass-transfer coefficient need to be measured or known. The dependence of activation energy on average moisture content on a dry basis (X) can be normalized as

$$\frac{\Delta E_v}{\Delta E_{v,b}} = f(\overline{X} - X_b) \quad (6)$$

where f is a function of water content difference, $\Delta E_{v,b}$ is the "equilibrium" activation energy representing the maximum ΔE_v determined by the relative humidity and temperature of the drying air

$$\Delta E_{v,b} = -RT_b \ln(RH_b) \quad (7)$$

RH_b is the relative humidity of drying air and T_b is the drying air temperature (K).

To generate the relative activation energy ($\Delta E_v/\Delta E_{v,b}$) shown by eq. 6, the activation energy (ΔE_v) can be evaluated by eq. 5 from one accurate drying experiment. So far, the experiments conducted to generate the relationship (eq. 6) generally used fairly dry air so the relationship covers a complete range of water content difference ($\overline{X} - X_b$), while X_b in the experiments for generating REA parameters is set to be very small value. Because eq. 6 is intended to describe the water removal that is restricted by solid matrix as well as to reflect the transition from the free water regime to the restricted regime, the experiment(s) that need to be performed for the REA must be covering the range toward equilibrium water content.

The activation energy is divided by the equilibrium activation energy ($\Delta E_{v,b}$) indicated by eq. 7 to yield the relative activation energy during drying. For similar drying condition and initial water content, it is possible to obtain the necessary REA parameters (apart from the equilibrium isotherm), expressed in the relative activation energy ($\Delta E_v/\Delta E_{v,b}$) as indicated in eq. 6 in one accurate drying experiment. The relative activation energy ($\Delta E_v/\Delta E_{v,b}$) generated can then be used to project to other drying conditions provided the material has the same initial moisture content.[33,50]

The Spatial Reaction Engineering Approach for Modeling Convective Drying of Mango Tissues

In this section, we describe the adaptation of L-REA to spatially distributed cases, that is, S-REA. Here, the experiments reported by Vaquiro et al.[15] which have been used to help establishing the REA, the samples were dried from three directions (x, y, and z directions), so 3-D modeling of the S-REA for convective and intermittent drying of mango tissues needs to be setup which is presented below.

The mass balance of water in the liquid phase (liquid water) is written as[24,27,29]

$$\frac{\partial(C_s X)}{\partial t} = \frac{\partial}{\partial x}\left(D_w \frac{\partial(C_s X)}{\partial x}\right) + \frac{\partial}{\partial y}\left(D_w \frac{\partial(C_s X)}{\partial y}\right) + \frac{\partial}{\partial z}(D_w \frac{\partial(C_s X)}{\partial z}) - \dot{I} \quad (8)$$

while the mass balance of water in the vapor phase (water vapor) is expressed as[24,27,29]

$$\frac{\partial C_v}{\partial t} = \frac{\partial}{\partial x}\left(D_v \frac{\partial C_v}{\partial x}\right) + \frac{\partial}{\partial y}\left(D_v \frac{\partial C_v}{\partial y}\right) + \frac{\partial}{\partial z}\left(D_v \frac{\partial C_v}{\partial z}\right) + \dot{I} \quad (9)$$

where X is the concentration of liquid water (kg H_2O kg dry solids^{-1}) and C_s is the solids concentration (kg dry solids m^{-3}) which can change if the structure is shrinking, $\dot{I}$ is the evaporation or condensation rate (kg H_2O m^{-3} s^{-1}) and $\dot{I}$ is >0 when evaporation occurs locally.

The heat balance is represented by the following equation[24,27,29]

$$\rho C_p \frac{\partial T}{\partial t} = \frac{\partial}{\partial x}\left(k \frac{\partial T}{\partial x}\right) + \frac{\partial}{\partial y}\left(k \frac{\partial T}{\partial y}\right) + \frac{\partial}{\partial z}\left(k \frac{\partial T}{\partial z}\right) - \dot{I}\,\Delta H_v \quad (10)$$

where T is the sample temperature (K).

The initial and boundary conditions for eqs. 8–10 are

$$t = 0, X = X_0, C_v = C_{v_0}, T = T_0 \quad \text{(initial condition, uniform initial concentrations and temperature)} \quad (11)$$

$$x = 0, y = 0, z = 0, \frac{dX}{dx} = 0, \frac{dC_v}{dx} = 0, \frac{dT}{dx} = 0 \quad \text{(symmetry boundary)} \quad (12)$$

$$x = L, y = L, z = L, -C_s D_w \frac{dX}{dx} = h_m \varepsilon_w \left(\frac{C_{v,s}}{\varepsilon} - \rho_{v,b}\right) \quad \text{(convective boundary for liquid water transfer)} \quad (13)$$

$$-D_v \frac{dC_v}{dx} = h_m \varepsilon_v \left(\frac{C_{v,s}}{\varepsilon} - \rho_{v,b}\right) \quad \text{(convective boundary for water vapor transfer)} \quad (14)$$

$$k \frac{dT}{dx} = h(T_b - T) \quad \text{(convective boundary for heat transfer)} \quad (15)$$

where ε_w and ε_v are fraction of surface area covered by liquid water and water vapor, respectively. Procedures to evaluate ε_w and ε_v are shown in Appendix B.

The sample dried was cube shape dried uniformly from all directions (x, y, and z directions)[15,47] so the mass balance of water in liquid phase can be simplified into[54,55]

$$\frac{\partial(C_s X)}{\partial t} = 3\frac{\partial}{\partial x}\left(D_w \frac{\partial(C_s X)}{\partial x}\right) - \dot{I} \tag{16}$$

while the mass balance of water in vapor phase can be expressed as

$$\frac{\partial C_v}{\partial t} = 3\frac{\partial}{\partial x}(D_v \frac{\partial C_v}{\partial x}) + \dot{I} \tag{17}$$

In addition, the heat balance can be represented as

$$\rho C_p \frac{\partial T}{\partial t} = 3\frac{\partial}{\partial x}\left(k\frac{\partial T}{\partial x}\right) - \dot{I}\,\Delta H_v \tag{18}$$

$\dot{I}$ is the local drying rate within the solid structure described as[44,45]

$$\dot{I} = h_{m_{in}} A_{in}(C_{v,s} - C_v) \tag{19}$$

where $h_{m,in}$ is the internal mass-transfer coefficient (m s^{-1}), A_{in} is the total internal surface area available for phase change (m^2), $C_{v,s}$ is the internal-solid-surface water vapor concentration (kg m^{-3}), and $C_{v,sat}$ is the internal-saturated water vapor concentration (kg m^{-3}).

By implementing the REA, internal-surface water vapor concentration can be written as[44,45]

$$C_{v,s} = \exp(\frac{-\Delta E_v}{RT})C_{v,sat} \tag{20}$$

Therefore, the local rate can be expressed as[44,45]

$$\dot{I} = h_{m_{in}} A_{in}\left(\exp\left(\frac{-\Delta E_v}{RT}\right)C_{v,sat} - C_v\right) \tag{21}$$

The relative activation energy of convective drying of mango tissues is generated from one accurate drying run of convective drying of mango tissues under constant environment conditions with the drying air temperature of 55°C.[15] The activation energy during drying is evaluated using eq. 5 and divided with the equilibrium activation energy represented in eq. 7 to yield the relative activation energy as mentioned in eq. 6. The relationship between the relative activation energy and average moisture content can be represented by simple mathematical equation obtained by least-square method using Microsoft Excel®.[56] The relative activation energy can be represented as

$$\frac{\Delta E_v}{\Delta E_{v,b}} = -9.92\times10^{-4}(\overline{X} - X_b)^3 + 9.74\times10^{-3}(\overline{X} - X_b)^2 - 0.101(\overline{X} - X_b) + 1.053 \tag{22}$$

The good agreement between the fitted and experimental relative activation energy is shown by R^2 of 0.999. Although the above equation involves X_b, as mentioned earlier, all successful applications of REA so far suggested that the experiments carried out should dry the materials to X_b of very small value to allow the correlations such as eq. 22 to cover the widest range of water content of practical interest. If X_b is close to initial water content, the activation energy calculated from the laboratory data can be misleading.

The relative activation energy correlated with eq. 22 has been implemented to model the convective and intermittent drying of mango tissues using the lumped reaction engineering approach (L-REA) and the results of modeling already matched well with the experimental data.[39,43] For modeling using the S-REA here, the relative activation energy shown in eq. 22 is used but the average moisture content $\overline{X}$ in eq. 22 is substituted by the local moisture content (X), as the REA is used to represent the local evaporation rate instead of the overall drying rate of the whole sample. In addition, it is emphasized that for the S-REA, the equilibrium relative activation energy ($\Delta E_{v,b}$) is evaluated at corresponding humidity and temperature inside the pores of the samples under equilibrium condition.

The effective vapor diffusivity is deduced from[57]

$$D_v = D_{v_o}\frac{\varepsilon}{\tau} \tag{23}$$

while D_{vo} is the water vapor diffusivity (m^2 s^{-1}), which is dependent on temperature, which can be expressed as[58]

$$D_{v_o} = 2.09\times10^{-5} + 2.137\times10^{-7}(T - 273.15) \tag{24}$$

The tortuosity (τ) of the samples is generally related to the porosity. The relationship can be represented as[59,60]

$$\tau = \varepsilon^{-n} \tag{25}$$

where n is the value between 0 and 0.5.[59,60] There is no noticeable effect of various values of n on the profiles of liquid water concentration, water vapor concentration and temperature as witnessed in many numerical tests performed in this study and $n = 0.5$ is chosen in this study.

C_s is the solid concentration which can be expressed by[26,43,44]

$$C_s = \frac{1-\varepsilon}{\frac{1}{\rho_s} + \frac{X}{\rho_w}} \tag{26}$$

while ε is the porosity, dependent on shrinkage and local moisture content. This can be determined according to[61]

$$\varepsilon = 1 - \frac{V_0}{V}(1-\varepsilon_0)\left(\frac{\frac{\rho_s}{\rho_w}\overline{X} + 1}{1 + \frac{\rho_s}{\rho_w}X_0}\right) \tag{27}$$

$h_{m,in}$ shown in eq. 19 is associated with the pore surfaces (porous media) or surfaces of the particles (packed beds) and internal to the sample being dried. Initially, the moisture is present in the void spaces of pores and within the pores. As drying proceeds, the moisture may migrate within the pores (on the pore surfaces) by liquid (surface) diffusion and from the surfaces of the pores through evaporation. Even at low water content, "surface" diffusion of liquid could occur along the pore surface accessible to air.[62] The internal mass-transfer coefficient shown in eq. 19 incorporates the restriction factor, as it may be affected by the pore structure and pore network inside the samples. This makes the value of $h_{m,in}$ grow from small value to the value of $\sim D_v/r_p$ (when constriction factor = 1).[26,48,49] In this study, $h_{m,in}$ of 0.01 m s^{-1} is chosen as it is in the order of D_v/r_p (hence deterministic) and application of

$h_{m,in}$ higher than this does not yield any noticeable difference in the profiles of moisture content and temperature.[44,45] The internal surface area (A_{in}) is evaluated according to the procedures outlined[29,44,45] based on the area of single cells inside the samples or particles and number of cells per unit volume inside the samples explained in Appendix C. The effective diffusivity of mango tissues presented by Vaquiro et al.[15] is expressed as

$$D_{\text{eff}} = 2.933 \times 10^{-3} \exp\left[-\frac{38.924 \times 10^3}{8.314T}\left(\frac{X}{X+1}\right)^{-1.885\times10^{-2}}\right] \tag{28}$$

Equation 28 can be used as an approximation to determine the liquid water diffusivity of mango tissues, but a little adjustment of the constant is needed to match the prediction with the experimental data of moisture content and temperature. The liquid water diffusivity used in this study can be expressed as

$$D_{\text{w}} = 2.933 \times 10^{-3} \exp\left[-\frac{31.924 \times 10^3}{8.314T}\left(\frac{X}{X+1}\right)^{-1.885\times10^{-2}}\right] \tag{29}$$

To yield the spatial profiles of moisture content, water vapor concentration and temperature of the convective of mango tissues, the mass and heat balances shown in eqs. 16–18 in conjunction with the initial and boundary conditions represented in eqs. 11–15, and the relative activation energy shown by eq. 22 are solved by method of lines.[63,64] By this method, the partial differential equations are transformed into a set of ordinary differential equations with respect to time by first discretizing the spatial derivatives. The ordinary differential equations are then solved simultaneously by *ode23s* in Matlab®.[65] The spatial derivative here is discretized into 10 increments; application of 200 increments has been conducted and there is no real difference in the profiles observed as shown in Figure 4. The shrinkage[43] is incorporated in the modeling by moving mesh in which the number of intervals is kept constant but the intervals of each increment are allowed to change according to the shrinkage relationship. Moving mesh was found to give better agreement toward experimental data than fixed coordinate (immobilizing boundary).[14]

The average moisture content of mango tissues during convective drying is evaluated by

$$\overline{X} = \frac{\int_0^{L(t)} X(x)dx}{\int_0^{L(t)} dx} \tag{30}$$

The profiles of average moisture content and center temperature are then validated against the experimental data of Vaquiro et al.[15]

The spatial reaction engineering approach for modeling convective drying of potato tissues

In the experiments reported by Srikiatden and Roberts[47] which are the subject of interest, the samples were covered at both top and bottom end to promote the 1-D drying condition with respect to radial direction,[47] so 1-D modeling (at radial direction) of the S-REA of the convective drying of cylindrical potato tissues is possible and can be represented by a set of equations of conservation below.

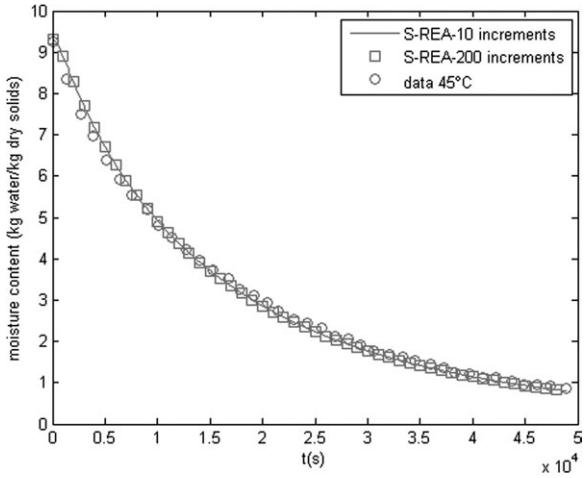

Figure 4. Moisture content profiles of convective drying of mango tissues at drying air temperature of 45°C solved with method of lines with 10 and 200 spatial increments.

The mass balance of liquid water can be represented as[24,27,29]

$$\frac{\partial(C_s X)}{\partial t} = \frac{1}{r}\frac{\partial}{\partial r}\left(D_w r \frac{\partial(C_s X)}{\partial r}\right) - \dot{I} \tag{31}$$

where X is the concentration of liquid water (kg H_2O kg dry solids^{-1}) and C_s is the solids concentration (kg dry solids m^{-3}), $\dot{I}$ is the evaporation or wetting rate (kg H_2O m^{-3} s^{-1}) and $\dot{I}$ is >0 when evaporation occurs locally.

The mass balance of water vapor can be expressed as[24,27,29]

$$\frac{\partial C_v}{\partial t} = \frac{1}{r}\frac{\partial}{\partial r}\left(D_v r \frac{\partial C_v}{\partial r}\right) + \dot{I} \tag{32}$$

where C_v is the concentration of water vapor (kg H_2O m^{-3}).

In addition the heat balance can be written as[24,27,29]

$$\rho C_p \frac{\partial T}{\partial t} = \frac{1}{r}\frac{\partial}{\partial r}\left(kr\frac{\partial T}{\partial r}\right) - \dot{I}\,\Delta H_v \tag{33}$$

where T is the sample temperature (K).

The initial and boundary conditions of eqs. 31–33 are

$$t = 0, X = X_o, C_v = C_{v_o}, T = T_o \quad \text{(initial condition, uniform initial concentrations and temperature)} \tag{34}$$

$$r = 0, \frac{dX}{dr} = 0, \frac{dC_v}{dr} = 0, \frac{dT}{dr} = 0 \quad \text{(symmetry condition)} \tag{35}$$

$$r = R, -C_s D_w \frac{dX}{dr} = h_m \varepsilon_w \left(\frac{C_{v,s}}{\varepsilon} - \rho_{v,b}\right) \quad \text{(convective boundary for liquid water transfer)} \tag{36}$$

$$-D_v\frac{dC_v}{dr}=h_m\varepsilon_v\left(\frac{C_{v,s}}{\varepsilon}-\rho_{v,b}\right)\quad\text{(convective boundary for water vapor transfer)}\quad(37)$$

$$k\frac{dT}{dr}=h(T_b-T)\quad\text{(convective boundary for heat transfer)}\quad(38)$$

Similar to the convective drying of mango tissues, the local evaporation rate ($\dot{I}$) and internal-solid-surface water vapor concentration are evaluated using eqs. 19–21. The relative activation energy of convective drying of potato tissues is generated from one accurate drying run of convective drying of potato tissues with the diameter of 1.4 cm at drying air temperature of 70°C.[47] The activation energy during drying was evaluated using eq. 5 based on the experimental data of moisture content and surface temperature during drying.[47] It is then divided with the equilibrium activation energy represented in eq. 7 to yield the relative activation energy as mentioned in eq. 6. The relationship between the relative activation energy and average moisture content can be represented by simple mathematical equation obtained by least-square method using Microsoft Excel®.[56] The relative activation energy can be represented as

$$\frac{\Delta E_v}{\Delta E_{v,b}}=\exp[-0.364(\overline{X}-X_b)^{0.876}]\quad(39)$$

For modeling using the S-REA, the average moisture content $\overline{X}$ in eq. 40 is substituted by the local moisture content (X) as the REA is then able represent the local evaporation or condensation rate here instead of the global drying rate. Similar to modeling for mango tissues, it is emphasized that for the S-REA, the equilibrium relative activation energy ($\Delta E_{v,b}$) is evaluated at corresponding humidity and temperature inside the pores under equilibrium condition.

Srikiatden and Roberts[47] reported the effective liquid diffusivity as

$$D_{eff}=1.0418\times10^{-5}\exp(-\frac{25.77\times10^3}{8.314T})\quad(41)$$

This was generated through isothermal drying experiments carefully arranged so the temperature dependence is correlated against the sample temperature. This is in contrast to many papers published in the literature. The real liquid diffusivity is, however, expected to be smaller than the effective diffusivity shown in eq. 41. This is due to that effective diffusivity expressed in eq. 41 is used to represent the totality of water transport (liquid diffusion, vapor diffusion, evaporation, and condensation). In this study, the sensitivity test is used to establish the best estimate of the liquid diffusivity. Equation 41 can still be used as the basis but is altered as

$$D_w=D_{w_0}\exp(-\frac{25.77\times10^3}{8.314T})\quad(42)$$

Here, the temperature dependence is preserved, which is a reasonable proposition. D_{w_0} is obtained by the numerical sensitivity test to match the predicted with the experimental data of moisture content and temperature. So far, no method has been presented anywhere in the literatures to measure the "pure liquid diffusivity" as such. In contrast, the vapor diffusivity in a structure can be made more definitive. The effective vapor diffusivity, tortuosity, solid concentration, and porosity are deduced from the procedure outlined above similar to that of the convective drying of the mango tissues. The same calculation procedures are used as that for the case of convective drying of mango tissues mentioned earlier. The spatial derivative is discretized into 10 increments; application of 200 increments has been conducted and there is no real differences in the profiles as indicated in Figure 5.

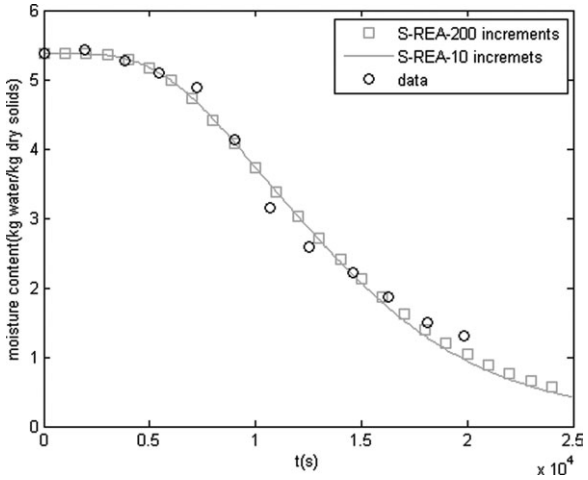

Figure 5. Moisture content profiles of convective drying of potato tissues with diameter of 1.4 cm solved with method of lines with 10 and 200 spatial increments.

The average moisture content in the core of potato tissues (X_{core}) is evaluated by

$$X_{core}=\frac{\int_0^{R_{core}}X(r)rdr}{\int_0^{R_{core}}rdr}\quad(43)$$

The average moisture content in cortex (X_{cortex}) is evaluated by

$$X_{cortex3}=\frac{\int_{R_{cortexin}}^{R_{sample\_out}}X(r)rdr}{\int_{R_{cortex\_in}}^{R_{cortex\_out}}rdr}\quad(44)$$

The results of modeling average moisture content in core and cortex (hence, the spatial distribution) are validated against the experimental data of Srikiatden and Roberts.[47]

Results and Discussion

Convective drying of mango tissues

The S-REA is used to model the convective drying of mango tissues at drying air temperature of 45, 55, and 65°C. The original formulation of the L-REA is implemented in the partial differential equation set for transport in porous media, to represent the local drying or condensation rate. Thus, it is coupled with the system of equations of conservation to describe the spatial profiles of moisture content, water vapor concentration, and temperature. It is noted that

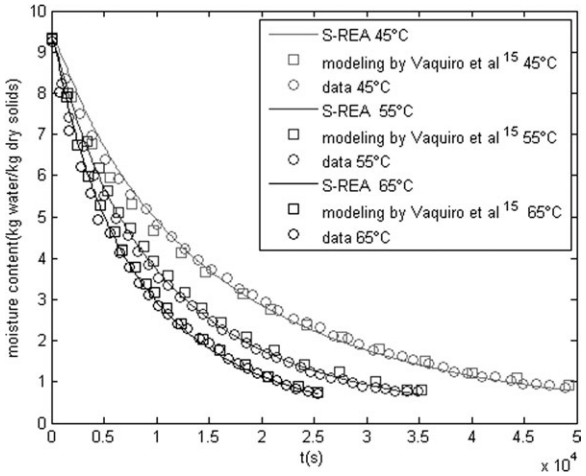

Figure 6. Average moisture content profiles of mango tissues during convective drying at different drying air temperatures.

if locally there is no vacant pore space which is connected with other pores or channels, the internal mass-transfer area should be considered to be zero; hence, the REA term is zero if the pores or channels are fully hydrated. In this study, the internal mass-transfer coefficient [$h_{m,in}$ (see eq. 19)] is chosen to 0.01 m s^{-1} as the sensitivity analysis indicates that $h_{m,in}$ is likely to be higher than 0.01 m s^{-1} but any higher than this does not give any noticeable difference in the profiles of moisture content and temperature predicted. More importantly, the value of 0.01 m s^{-1} is also in the order of D_v/r_p,[44,45] thus, it is a fundamental value.

The good agreement between the predicted and experimental data of the average moisture content and the center temperature are shown in Figures 6 and 7. It is also supported by R^2 of moisture content higher than 0.996 and R^2 of temperature higher than 0.985 as listed in Table 2. The results of the S-REA modeling match well with the experimental data. Benchmarks against diffusion-based model[15] indicate that the S-REA yields comparable or even better agreement toward the experimental data.

Figure 8 shows the spatial profiles of moisture content of convective drying of mango tissues at drying air temperature

Table 2. R^2 and *RMSE* of Convective Drying of Mango Tissues

Drying Air Temperature (°C)	R^2 for X	*RMSE* for X	R^2 for T	*RMSE* for T
45	0.998	0.103	0.998	0.285
55	0.999	0.079	0.985	1.004
65	0.996	0.150	0.994	0.842

of 45°C. The moisture content at the outer part of the samples is lower than that at the inner part which indicates the effect of moisture removal. Initially, the gradient of moisture content inside the samples is relatively high but this decreases as the drying progresses. At the end of drying, no noticeable gradient of moisture content is observed which indicates the equilibrium moisture content is nearly approached. If no liquid diffusion mechanism is used, the S-REA model would not be able to project this kind of liquid water profiles.[44,45]

The S-REA can generate the spatial profiles of water vapor concentration. The spatial profiles of water vapor concentration of convective drying of mango tissues at drying air temperature of 45°C are shown in Figure 9. The profiles of water vapor concentration are significantly affected by the local composition and structure of the samples being dried. Along drying, the concentration of water vapor achieves maximum at particular position inside the samples. This could be because at the core of samples, the moisture content is higher than that of the outer part which makes the porosity of the core of samples smaller than that of the outer part. The lower porosity retards the evaporation rate at the sample core. At the outer part of the samples, the water extraction rate may be enhanced because of higher porosity but this seems to be balanced by high-diffusive water vapor transfer, as a result of higher porosity and higher temperature at the outer part of the samples. The S-REA seems to capture this physics well and can model the profiles of water vapor concentration well qualitatively.

The spatial profiles of temperature are presented in Figure 10. The temperature of the outer part of the samples is higher than that of the inner part because the samples receive heat by convection from the drying air and it is used for vaporization and if any "left" as such, it would further

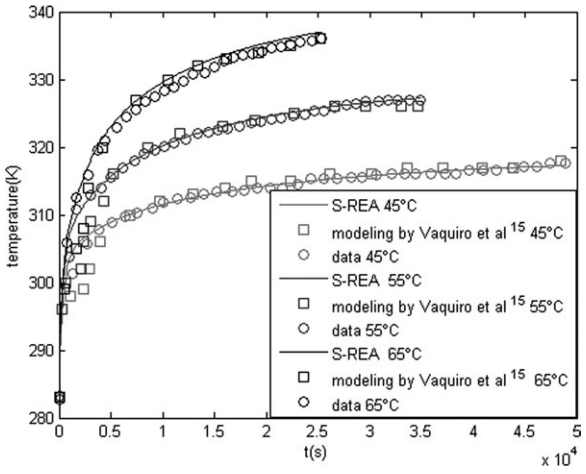

Figure 7. Center temperature profiles of mango tissues during convective drying at different drying air temperatures.

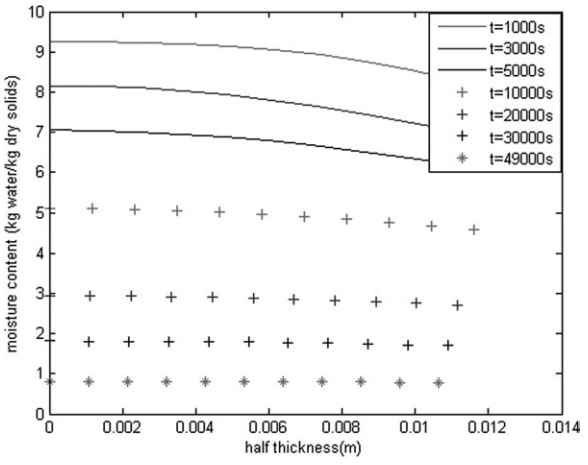

Figure 8. Spatial moisture content profiles of mango tissues during convective drying at drying air temperatures of 45°C.

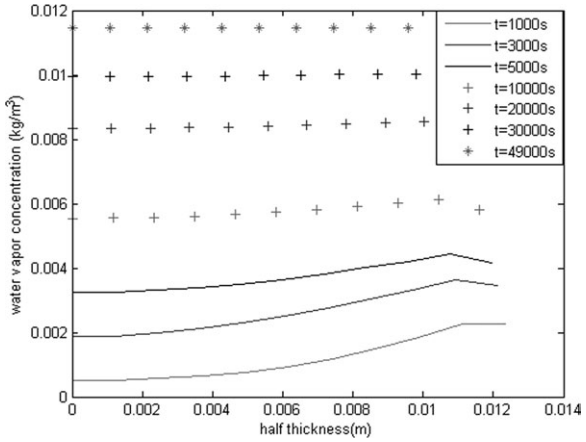

Figure 9. Spatial water vapor concentration profiles of mango tissues during convective drying at drying air temperatures of 45°C.

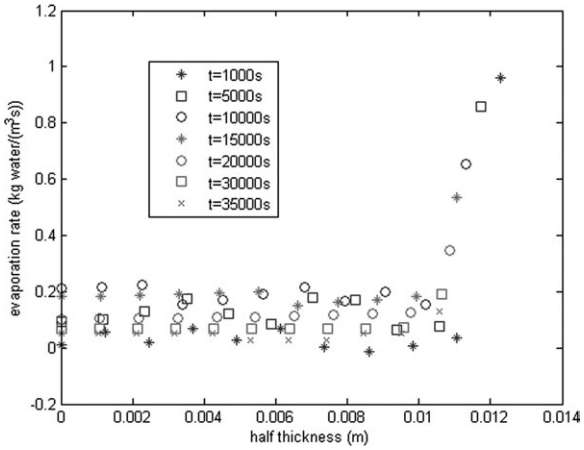

Figure 11. Profiles of evaporation rate inside mango tissues during convective drying at drying air temperature of 55°C.

penetrate inward by conduction. However, the gradient of temperature inside the samples is not large which may indicate that the temperature inside the samples is essentially uniform. This is in agreement with the prediction of Chen–Biot number (*Ch_Bi*),[43,52] which remains low (less than 0.3) during drying reported previously.[43]

Figure 11 indicates the local evaporation rate inside mango tissues during convective drying at drying air temperature of 55°C. As drying proceeds, the evaporation rate at the inner part is smaller than that of the outer part which could be due to high moisture content at the inner part of the sample. This means a lower porosity there that retards the evaporation rate. The observation is also in agreement with the intuitive explanation of profiles of water vapor concentration during drying by Chen.[66] As drying progresses, the evaporation rate increases as the temperature increases. However, the increase is observed up to drying time around 15,000 s. After this period, the evaporation rate decreases as the moisture content inside the samples is depleted. At the end of drying, essentially there is no much difference in evaporation rate inside the samples because the moisture content has nearly achieved equilibrium, under the drying conditions.

Therefore, it can be said that the S-REA approach models the convective drying of mango tissues well, and the original REA is a simple alternative approach to represent the local evaporation and condensation rate. In addition, the S-REA has been easily operated to yield the profiles of water vapor concentration, local evaporation rate, and local heat evaporation rate inside the mango tissues during drying.

Convective drying of potato tissues

As mentioned earlier, the S-REA has also been implemented to model the convective drying of potato tissues. The relative activation energy is generated from one accurate drying run which is the convective drying at air temperature of 70°C. It is represented in eq. 39. Similar to the convective drying of mango tissues, the internal mass-transfer coefficient [$h_{m,in}$ (on eq. 19)] is chosen to be 0.01 m s^{-1} as the sensitivity analysis indicates that $h_{m,in}$ of higher than 0.01 m s^{-1} does not give any noticeable differences in the profiles of moisture content and temperature. Nicely, this is also in the order of D_v/r_p as suggested by Kar and Chen;[44,45] hence, $h_{m,in}$ is a fundamental value. However, D_{w_0} (on eq. 42) is determined by sensitivity analysis and it is found that D_{w_0} of 6.5×10^{-6} m^2 s^{-1} gives the best agreement against the experimental data. It is emphasized that the temperature dependence function for the liquid diffusivity in this case was

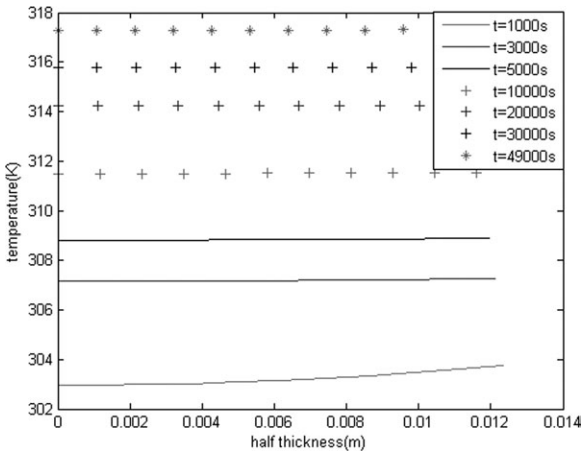

Figure 10. Spatial temperature profiles of mango tissues during convective drying at drying air temperatures of 45°C.

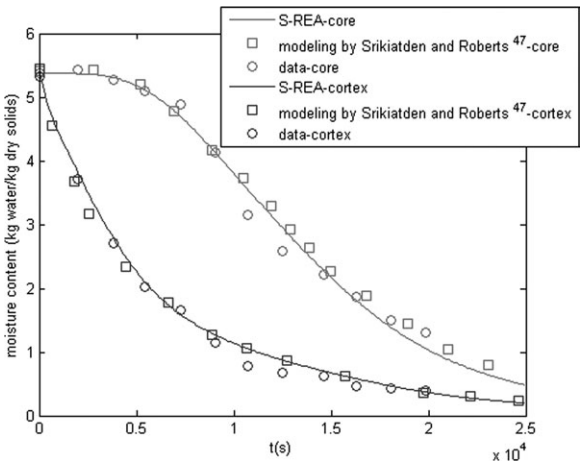

Figure 12. Moisture content profiles in core and cortex during convective drying of potato tissues with diameter of 1.4 cm

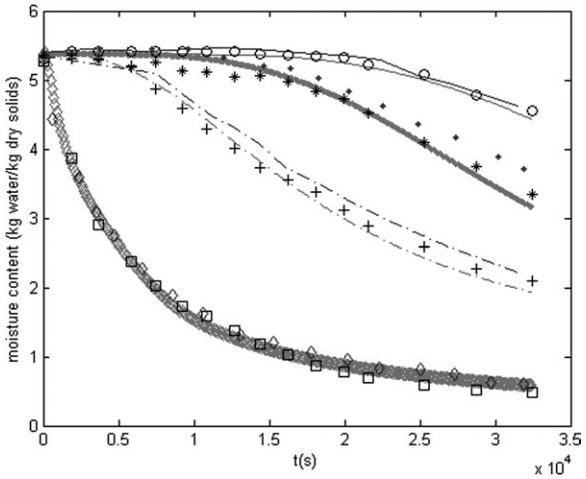

Figure 13. Moisture content profiles in core and cortex during convective drying of potato tissues with diameter of 2.8 cm − red S-REA core, · red S-REA cortex 1, − red S-REA cortex 2, ◇ red S-REA cortex 3 − blue modeling by Srikiatden and Roberts[47] core, · blue modeling by Srikiatden and Roberts[47] cortex 1, · blue modeling by Srikiatden and Roberts[47] cortex 2, ◇ blue modeling by Srikiatden and Roberts[47] cortex 3 ○ data core, * data cortex 1, + data cortex 2, □ data cortex 3.

obtained in isothermal drying experiments specially designed by Srikiatden and Roberts,[48] in contrast to many studies published in literatures that the diffusivity in the material is related to drying air temperature instead.[24]

Results of modeling of convective drying of potato tissues are shown in Figures 12–14. Figure 12 shows the profiles of moisture content of each part of potato cylindrical tissues with the diameter of 1.4 cm during the convective drying. It can be shown that the results of modeling match well with the experimental data with correlation coefficient R^2 of 0.98. Benchmarks against modeling implemented by Srikiatden and Roberts[47] with the liquid diffusivity concept indicate that the S-REA yields comparable results.

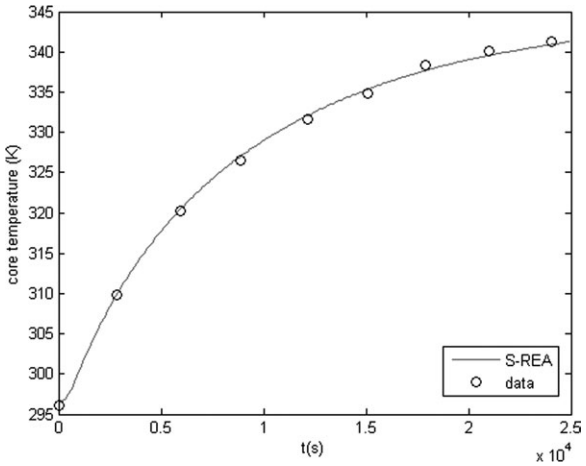

Figure 14. Core temperature profiles during convective drying of potato tissues with diameter of 1.4 cm.

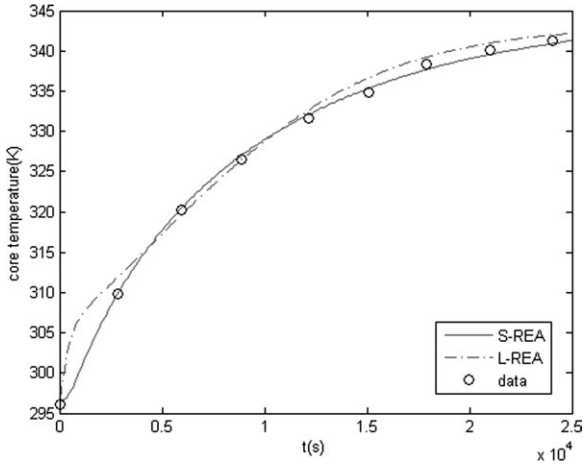

Figure 15. Comparison of core temperature profiles during convective drying of potato tissues with diameter of 1.4 cm predicted using S-REA and L-REA.

In addition, the profiles of moisture content of each part of samples with the diameter of 2.8 cm are shown in Figure 13. Again, a good agreement toward the experimental data is observed (R^2 of 0.992). Indeed, the S-REA describes the moisture content profiles accurately during convective drying of potato tissues the diameter of 2.8 cm. Benchmarks toward modeling implemented by Srikiatden and Roberts[47] indicate that the REA yields comparable or even better results. It can be said that the S-REA can be used to model the profiles of moisture content very well.

Figure 14 indicates the core temperature during convective drying of potato tissues with the diameter of 1.4 cm. The predictions of temperature using the S-REA match well with the experimental data with R^2 of 0.99. Benchmarks against modeling implemented by Srikiatden and Roberts[47] indicate that the S-REA yields comparable results. Overall, S-REA seems to be a sound approach to model the details of spatial distributions of temperature, liquid water, and water vapor concentration in the material being dried.

Figure 15 shows the comparisons of the core temperature during drying of potato tissues with the diameter of 1.4 cm predicted by the S-REA and L-REA. By the combination with the approximation of temperature distribution inside the samples,[43] the L-REA predicts the core temperature reasonably well. The L-REA results in a slight overestimation of core temperature at the beginning of drying. The S-REA models the core temperature very well; the slight overestimation at the beginning of drying is not observed by the S-REA. Nevertheless, the distinct advantage of the S-REA over the L-REA is the local moisture content, concentration of water vapor, and temperature that can be predicted, thus, it gives better understanding of transport phenomena of drying.

Conclusions

In this article, the S-REA is used as nonequilibrium multiphase mass-transfer model to describe drying of food and biological materials. The basic, original REA formulation is used to describe the local evaporation and condensation rate. This is then incorporated with the standard mechanistic energy and mass-transfer equation sets to model the convective drying. The relative activation energy as the fingerprint

of drying of one particular material, which is implemented in the L-REA, is generated from one accurate drying run of a sample of the same material. The predictability of the REA model lies on the fact that the parameters obtained from one condition may be used to project other different conditions. Solving a set of differential equations of conservation yields the spatial profiles of moisture content, water vapor concentration, and temperature. The local rate of evaporation/condensation is also linked to the local exposed pore/liquid surface which is a local structural parameter. As such, the microstructural aspect may also be incorporated in near future. In any case, the results of modeling using the S-REA in this study match well with the experimental data. The S-REA also yields the profiles of water vapor concentration and evaporation/condensation rate during drying, which gives better understanding of transport phenomena of drying. Based on this study, it is revealed that the S-REA can model the convective drying of food and biological materials very well. The S-REA can be made as an accurate model of the nonequilibrium multiphase transport during drying. A significant contribution of the development of REA for describing the transport phenomena of drying processes has thus been made here.

Acknowledgments

The first author acknowledges ALAS (Australian Leadership Award Scholarship).

Notation

A = surface area of samples, m^2
A_{in} = internal surface area, m^2
A_o = initial surface area of samples, m^2
A_p = cell surface area, m^2
C_p = specific heat of sample, J kg^{-1} K^{-1}
C_{pmix} = specific heat of mixture, J kg^{-1} K^{-1}
C_{ps} = specific heat of solids, J kg^{-1} K^{-1}
C_{pw} = specific heat of water, J kg^{-1} K^{-1}
C_s = solid concentration, kg m^{-3}
C_v = water vapor concentration, kg m^{-3}
$C_{v,s}$ = internal-surface vapor concentration, kg m^{-3}
$C_{v,sat}$ = internal-saturated vapor concentration, kg m^{-3}
D_v = effective water vapor diffusivity, m s^{-2}
$D_{v,o}$ = water vapor diffusivity, m s^{-2}
D_w = capillary diffusivity, m s^{-2}
h = heat-transfer coefficient, W m^{-2} K^{-1}
h_m = mass-transfer coefficient, m s^{-1}
$h_{m,in}$ = internal mass-transfer coefficient, m s^{-1}
I = local evaporation rate, kg m^{-2} s^{-1}
k = thermal conductivity of sample, W m^{-1} K^{-1}
m_p = dry mass of cell, kg
m_s = dried mass sample of material, kg
m_w = mass of liquid water, kg
m_v = mass of water vapor, kg
n = constant
N = number of cell in samples
n_p = number of cell per unit volume, m^{-3}
r = radial position, m
RH_b = relative humidity of drying air
r_p = cell radius, m
T = sample temperature, K
T_s = surface sample temperature, K
t = time, s
T_b = drying air temperature, K
V = volume of sample, m^3
V_p = cell volume, m^3
w = mass fraction of water
X = moisture content on dry basis, kg kg^{-1}
$\overline{X}$ = average moisture content on dry basis, kg kg^{-1}
X_b = equilibrium moisture content on dry basis, kg kg^{-1}
X_o = initial moisture content, kg kg^{-1}
ΔE_v = apparent activation energy, J mol^{-1}
$\Delta E_{v,b}$ = "equilibrium" activation energy, J mol^{-1}
ΔH_v = vaporization heat of water, J kg^{-1}
ε = porosity
ε_w = fraction by liquid water
ε_v = fraction by water vapor
ε_o = initial porosity
Θ = constriction factor
ρ = sample density, kg m^{-3}
ρ_s = density of solids, kg m^{-3}
$\rho_{v,b}$ = vapor concentration in drying medium, kg m^{-3}
$\rho_{v,s}$ = surface vapor concentration, kg m^{-3}
$\rho_{v,sat}$ = saturated vapor concentration, kg m^{-3}
ρ_w = density of water, kg m^{-3}
τ = tortuosity

Literature Cited

1. Gunasekaran S, Pulsed microwave-vacuum drying of food. *Drying Technol*. 1999;17:395–412.
2. Chou SK, Chua KJ, Mujumdar AS, Hawlader MNA, Ho JC. On the intermittent drying of an agricultural product. *Trans IChemE Part C*. 2000;78:193–203.
3. Tan M, Chua KJ, Mujumdar, AS, Chou S. Osmotic dehydration of potato and pineapple: effect of intermittent radiation and continuous convection in a heat pump dryer. *Drying Technol*. 2001;19: 2193–2207.
4. Ho JC, Chou SK, Mujumdar AS, Hawlader MNA. Analytical study of cyclic temperature drying: effects on drying kinetics and product quality. *J Food Eng*. 2002;51:65–75.
5. Chua KJ, Mujumdar AS, Chou SK. Intermittent drying of bioproducts—an overview, *Bioresour Technol*. 2003;90:285–295.
6. Li YB, Cao CW, Yu QL, Zhong QX. Study on rough rice fissuring during intermittent drying. *Drying Technol*. 1999;17:1779–1793.
7. Cihan A, Ece MC. Liquid diffusion model for intermittent drying of rough rice. *J Food Eng*. 2001;49:327–331.
8. Yang W, Jia CC, Siebenmorgen TJ, Pan Z, Cnossen AG. Relationship of kernel moisture content gradients and glass transition temperatures to head rice yield. *Biosystems Eng*. 2003;85: 467–476.
9. Kowalski SJ, Pawlowski, A. Drying of wet materials in intermittent conditions, *Drying Technol*. 2010;28:636–643.
10. Kowalski SJ, Pawlowski A. Modeling of kinetics in stationary and intermittent drying, *Drying Technol*. 2010;28:1023–1031.
11. Azzouz S, Guizani A, Jomaa W, Belghith, A. Moisture diffusivity and drying kinetic equation of convective drying of grapes. *J Food Eng*. 2002;55:323–330.
12. Pakowski Z, Adamski A. The comparison of two models of convective drying of shrinking materials using apple tissue as an example. *Drying Technol*. 2007;25:1139–1147.
13. Mariani VC, de Lima AGB, Coelho LS. Apparent thermal diffusivity estimation of the banana during drying using inverse method, *J Food Eng*. 2008;85:569–579.
14. Thuwapanichayanan R, Prachayawarakorn S, Soponronnarit S. Modeling of diffusion with shrinkage and quality investigation of banana foam mat drying, *Drying Technol*. 2008;26:1326–1333.
15. Vaquiro HA, Clemente G, Garcia Perez JV, Mulet A., Bon J. Enthalpy driven optimization of intermittent drying of *Mangifera indica* L. *Chem Eng Res Des*. 2009;87:885–898.
16. Cihan A, Ece MC. Liquid diffusion model for intermittent drying of rough rice. *J Food Eng*. 2001;49:327–331.
17. Trujillo FJ, Wiangkaew C, Pham QT. Drying modeling and water diffusivity in beef meat, *J Food Eng*. 2007;78:74–85
18. Hacihafizoglu O, Cihan A, Kahveci K, de Lima, AGB. A liquid diffusion model for thin-layer drying of rough rice. *Eur Food Res Technol*. 2008;226:787–793.
19. Ramos IN, Miranda JMR, Brandao TRS, Silva CLM. Estimation of water diffusivity parameters on grape dynamic drying. *J Food Eng*. 2010;97:519–525.
20. Nguyen TA, Verboven P, Scheerlinck N, Vandewalle S, Nicolai BM. Estimation of effective diffusivity of pear tissue and cuticle by means of a numerical water diffusion model, *J Food Eng*. 2006; 72:63–72
21. Batista LM, da Rosa CA, Pinto LAA. Diffusive model with variable effective diffusivity considering shrinkage in thin layer drying of chitosan. *J Food Eng*. 2007;81:127–132.

22. Corzo O, Bracho N, Alvarez C. Water effective diffusion coefficient of mango slices at different maturity stages during air drying. *J Food Eng*. 2008;87:479–484.
23. Roberts JS, Kidd DR, Padilla-Zakour O. Drying kinetics of grape seeds. *J Food Eng*. 2008;89:460–465.
24. Chen XD. Moisture diffusivity in food and biological materials. *Drying Technol*. 2008;25:1203–1213.
25. Crank J. *The Mathematics of Diffusion*, Oxford: Clarendon Press, 1975.
26. Kar S. Drying of porcine skin-theoretical investigations and experiments. Ph.D. thesis. Monash University, Australia. 2008.
27. Zhang J, Datta AK. Some considerations in modeling of moisture transport in heating of hygroscopic materials. *Drying Technol*. 2004;22:1983–2008.
28. Datta, AK. Porous media approaches to studying simultaneous heat and mass transfer in food processes. I: Problem formulations. *J. Food Eng*. 2007;80:80–95.
29. Chong, LV, Chen, XD. A mathematical model of the self-heating of spray-dried food powders containing fat, protein, sugar and moisture. *Chem Eng Sci*. 1999;54:4165–4178.
30. Scarpa D, Milano G. The role of adsorption and phase change phenomena in the thermophysical characterization of moist porous materials, *Int J Thermophys*. 2002;23:1033–1046.
31. Chen XD, Xie GZ. Fingerprints of the drying behavior of particulate or thin layer food materials established using a reaction engineering model. *Trans IChemE, Part C: Food Bioprod Proc*. 1997;75: 213–222.
32. Chen XD, Pirini W, Ozilgen M. The reaction engineering approach to modeling drying of thin layer pulped kiwifruit flesh under conditions of small Biot numbers. *Chem Eng Proc*. 2001;40:311–320.
33. Chen XD, Lin SXQ. Air drying of milk droplet under constant and time dependent conditions. *AIChE J*. 2005;51:1790–1799.
34. Lin SXQ, Chen XD. A model for drying of an aqueous lactose droplet using the reaction engineering approach. *Drying Technol*. 2006;24:1329–1334.
35. Lin SXQ, Chen XD. Prediction of air drying of milk droplet under relatively high humidity using the reaction engineering approach. *Drying Technol*. 2005;23:1396–1406.
36. Lin SXQ, Chen, XD. The reaction engineering approach to modeling the cream and whey protein concentrate droplet drying. *Chem Eng Proc*. 2007;46:437–443.
37. Putranto A, Chen XD, Webley, PA. Infrared and convective drying of thin layer of polyvinyl alcohol (PVA)/glycerol/water mixture—the reaction engineering approach (REA), *Chem Eng Proc: Process Intensification*. 2010;49:348–357.
38. Putranto A, Chen XD, Webley PA. Application of the reaction engineering approach (REA) to model cyclic drying of polyvinyl alcohol (PVA)/glycerol/water mixture, *Chem Eng Sci*. 2010;65: 5193–5203.
39. Putranto A, Xiao Z, Chen, XD, Webley, PA. Intermittent drying of mango tissues: implementation of the reaction engineering approach (REA), *Ind Eng Chem Res*. 2010;50:1089–1098.
40. Putranto A, Chen XD, Xiao Z, Webley PA. Modeling of high-temperature treatment of wood by using the reaction engineering approach (REA), *Bioresour Technol*. 2010;102:6214–6220.
41. Putranto A, Chen, XD, Devahastin S, Xiao Z, Webley PA. Application of the reaction engineering approach (REA) to model intermittent drying under time-varying humidity and temperature, *Chem Eng Sci*. 2010;66:2149–2156.
42. Putranto A, Chen XD, Zhou W. 2011. Modeling of baking of cake using the reaction engineering approach (REA), *J Food Eng*. 2011;105:638–646.
43. Putranto A, Chen XD, Webley PA. Modeling of drying of thick samples of mango and apple tissues using the reaction engineering approach (REA), *Drying Technol*. 2011;29:961–973.
44. Kar S, Chen, XD. Moisture transport across porcine skin: experiments and implementation of diffusion-based models, *Int J Healthcare Technol Manage*. 2010;11:474–522
45. Kar S, Chen, XD. Modeling of moisture transport across porcine skin using reaction engineering approach and examination of feasibility of the two phase approach. *Chem Eng Commun*. 2011;198: 847–885.
46. Sanjuan N, Lozano M, Garcia-Pascual P, Mulet A. Dehydration kinetics of red pepper (*Capsicum annuum* L var Jaranda). *J Sci Food Agric*. 2004;83:697–701.
47. Srikiatden J, Roberts JS. Predicting moisture profiles in potato and carrot during convective hot air drying using isothermally measured effective diffusivity. *J Food Eng*. 2008;84:516–525.
48. Srikiatden J, Roberts JS. Measuring moisture diffusivity of potato and carrot (core and cortex) during convective hot air and isothermal drying. *J Food Eng*. 2006;74:143–152.
49. Roberts JS, Tong CH, Lund DB. Drying kinetics and time-temperature distribution of pregelatinized bread, *J Food Sci*. 2002;67: 1080–1087.
50. Chen XD. The basics of a reaction engineering approach to modeling air drying of small droplets or thin layer materials, *Drying Technol*. 2008;26:627–639.
51. Keey RB. *Drying of Loose and Particulate Materials*, New York: Hemisphere Publishing, 1992.
52. Chen XD, Peng XF. Modified Biot number in the context of air drying of small moist porous objects, *Drying Technol*. 2005;23:83–103.
53. Patel KC, Chen XD. Surface-center temperature differences within milk droplets during convective drying and drying-based Biot number analysis, *AIChE J*. 2008;54:3273–3290.
54. Incropera FP, DeWitt DP. *Fundamentals of Heat and Mass Transfer*, 5th ed. New York: Wiley, 2002.
55. Van der Sman RGM. Simple model for estimating heat and mass transfer in regular shaped foods. *J Food Eng*. 2003;60:61–76.
56. Microsoft Corp., 2012. office.microsoft.com/en-au/excel, accessed on 14 March 2012
57. Bird RB, Stewart WE, Lightfoot EN. *Transport Phenomena*, 2nd international ed. New York: Wiley, 2002.
58. Slattery JC, Bird, RB. Calculation of the diffusion coefficient of dilute gases and of the self diffusion coefficient of dense gases. *AIChE J*. 1958;4:137–142.
59. Audu TOK, Jeffreys GV. The drying of drops of particulate slurries. *Trans IChemE Part A*. 1975;53:165–175.
60. Gimmi T, Fuhler H, Studer B, Rasmuson A. Transport of volatile chlorinated hydrocarbons in unsaturated aggregated media. *Water Air Soil Pollut*. 1993;68:291–305.
61. Madiouli J, Lecomte D, Nganya T, Chavez S, Sghaier J, Sammouda H. A method for determination of porosity change from shrinkage curves of deformable materials, *Drying Technol*. 2007;25:621–628.
62. Chen XD, Mujumdar, AS. *Drying Technologies in Food Processing*. UK: Blackwell Publishing, 2008.
63. Constantinides A, *Numerical Methods for Chemical Engineers with MATLAB applications*. Upper Saddle River, N.J.: Prentice Hall PTR, 1999.
64. Chapra SC. *Numerical Methods for Engineers*. Boston: McGraw-Hill, 2006.
65. Mathworks, 2012. www.mathworks.com, accessed on 14 March 2012.
66. Chen, XD *Simultaneous Heat and Mass Transfer*. *In Handbook of Food and Bioprocess Modeling Techniques*. Sablani S, Rahman S, Datta AL, Mujumdar AS. (Eds.) Boca Raton, FL: CRC Press, 2007.
67. Calivano NA, Calvelo A. Thermal conductivity of potato between 50 and 100 °C. *J Food Sci*. 1991;56:586–587.
68. Wang N, Brennan, JG. Moisture sorption isotherm characteristics of potatoes at four temperatures. *J Food Eng*. 1991;14:269–287.
69. Wang N, Brennan, JG. The influence of moisture content and temperature on the specific heat of potato measured by differential scanning calorimetry. *J Food Eng*. 1993;19:303–310.
70. Zogzas NP, Maroulis, ZB, Marinos-Kouris D. Densities, shrinkage and porosity of some vegetables during air drying. *Drying Technol*. 1994;12:1653–1666.
71. Ousegui A, Moresoli C, Dostie M, Marcos B. Porous multiphase approach for baking process—explicit formulation of evaporation rate, *J Food Eng*. 2010;100:535–544.

Appendix A: Properties of potato tissues[48,67–70]

$$\rho_w = 997 + 3.14 \times 10^{-3}(T - 273.15) - 3.76 \times 10^{-3}(T - 273.15)^2 \quad \text{(A1)}$$

$$\rho_s = 1480 \quad \text{(A2)}$$

$$\rho = \frac{1 + X}{\frac{1}{\rho_s} + \frac{X}{\rho_w}} \quad \text{(A3)}$$

$$k = 1.05 - 1.96 \times 10^{-2}(T - 273.15) + 1.9 \times 10^{-4}(T - 273.15)^2 \quad \text{(A4)}$$

$$X_b = 0.029 \frac{15.975 RH_b}{(1 - 0.9 RH_b)(1 + 15.075 RH_b)} \quad \text{(A5)}$$

Appendix B: Evaluation of fraction of surface area covered by liquid water (ε_w) and that by water vapor (ε_v)[71]

$$\frac{m_w}{V} = C_s X = \rho_w \varepsilon_w \quad \text{(B1)}$$

$$\frac{m_v}{V} = \rho_v \varepsilon_v \quad \text{(B2)}$$

Appendix C: Evaluation of internal surface area (A_{in})[44–45]

$$A_p = 4\pi {r_p}^2 \quad \text{(C1)}$$

$$V_p = \frac{4}{3}\pi {r_p}^3 \quad \text{(C2)}$$

$$m_p = \rho_p V_p (1 - v_w) \quad \text{(C3)}$$

$$N = \frac{m_s}{m_p} \quad \text{(C4)}$$

$$n_p = \frac{N}{V_s} \quad \text{(C5)}$$

$$A_{in} = n_p A_p \quad \text{(C6)}$$

Manuscript received Oct. 17, 2011, and revision received Mar. 17, 2012.